

The Onsager principle and physics preserving numerical schemes*

Huangxin Chen[†]

Hailiang Liu[‡]

Xianmin Xu[§]

Abstract

We present a natural framework for constructing energy-stable time discretization schemes. By leveraging the Onsager principle, we demonstrate its efficacy in formulating partial differential equation models for diverse gradient flow systems. Furthermore, this principle provides a robust basis for developing numerical schemes that uphold crucial physical properties. Within this framework, several widely used schemes emerge naturally, showing its versatility and applicability.

Key words. Onsager principle, dissipative physical systems, physics preserving, optimization

MSC codes. 65M12, 65M22, 76M30

1 Introduction

Physical systems inherently exhibit critical properties such as energy dissipation relations, mass conservation, and positive densities. It is imperative to design numerical schemes that preserve these fundamental characteristics to accurately model and simulate such systems. The recent surge in interest within the numerical analysis community to develop physics-preserving numerical methods reflects the importance of maintaining these essential properties in simulation techniques. For numerical approximations of dissipative physical systems, a central challenge lies in devising methods that satisfy critical system properties such as energy dissipation laws, mass conservation and preservation of solution positivity or boundedness. Notable approaches include the convex splitting method [11, 36], linear stabilization methods [39, 41], exponential time-differencing schemes [2, 4, 13, 8], as well as recent advancements like the invariant energy quadratization (IEQ) [44, 45] and scalar auxiliary variable (SAV) approaches [37, 38]. Specifically, for structure-preserving numerical methods applied to systems such as the Planck-Nernst-Poisson system and Fokker-Planck equations, the energetic variational approach has proven effective [10, 21, 9], and one can also refer to other energy dissipative schemes such as in [31, 24, 14, 15, 32] and the references therein. This paper explores physics-preserving numerical methods for dissipative physical systems from a fresh perspective grounded in the Onsager principle.

The Onsager principle, a fundamental law in thermodynamic physics [29, 30], has played a crucial role as a modeling tool in various soft matter problems [6]. In recent years, it has been employed not only as a modeling tool but also as an approximation tool for deriving reduced models [7, 28, 43], as well as in the development of numerical methods [27, 42, 40, 26], among other applications. This endeavor faces two central challenges: (1) Selecting appropriate

*The work of Huangxin Chen was partially supported by National Key Research and Development Project of China (Grant No. 2023YFA1011702) and National Natural Science Foundation of China (Grant No. 12122115). The work of Xianmin Xu was partially supported by National Natural Science Foundation of China (Grant No. 11971469 and No. 12371415) and by Beijing Natural Science Foundation (Grant No. Z240001).

[†]School of Mathematical Sciences and Fujian Provincial Key Laboratory on Mathematical Modeling and High Performance Scientific Computing, Xiamen University, Fujian, 361005, China (chx@xmu.edu.cn).

[‡]Iowa State University, Department of Mathematics, Ames, IA 50011, United States (hliu@iastate.edu)

[§]Corresponding author. LSEC, ICMSEC, NCMIS, Academy of Mathematics and Systems Science, Chinese Academy of Sciences, Beijing 100190, China (xmxu@lsec.cc.ac.cn)

slow variables to effectively apply the Onsager principle; (2) Determining the numerous free coefficients in the structured dynamical system. The present study specifically addresses the utilization of the Onsager principle to derive a natural time discretization for equations of interest.

The Onsager principle extends the Rayleigh's principle of the least energy dissipation in Stokesian hydrodynamics and is a well-established model for the dynamics of dissipative systems near equilibrium. To elucidate the Onsager principle, we initiate the explanation by considering an ordinary differential system with gradient flow structure. Given the generalized coordinates $y = (y_1, \dots, y_s)^\top$, their dynamical evolution is described by the equation

$$A\dot{y} = -\nabla U(y),$$

where we use the dot for the time derivative, $\dot{y} = \partial_t y$, U represents a potential function. The matrix A characterizes the energy dissipation in the system and is positive semi-definite, satisfying $y \cdot Ay \geq 0$ for all y . A key insight from Onsager establishes that if the system exhibits microscopic time reversibility, then A is symmetric ($A = A^\top$). This reciprocal relation allows us to express the above time evolution equation as a variational principle. Introducing the Rayleighian

$$R = \Phi + \dot{U}, \quad (1)$$

where Φ is defined by

$$\Phi = \frac{1}{2} \|z\|_A^2 := \frac{1}{2} z \cdot Az, \quad z = \dot{y}$$

and \dot{U} is defined by

$$\dot{U} = \nabla U \cdot \dot{y}.$$

The force balance equation is equivalent to the condition $\nabla_y R = 0$. In other words, the evolution of y is determined by the requirement that R is minimized with respect to \dot{y} . This is the essence of the Onsager principle.

Now, let's employ the same principle to discretize the equation. We straightforwardly adopt a discrete form of R :

$$\Phi(z) + \frac{U(y) - U(y_k)}{\tau},$$

subject to

$$z = \frac{y - y_k}{\tau}.$$

Here, τ represents the time step, and y_k is the solution update at time $t_k = k\tau$. With a fixed time step, we can determine y_{k+1} by solving a constraint optimization problem:

$$\begin{aligned} y_{k+1} &= \operatorname{argmin}_{y,z} \left\{ \Phi(z) + \frac{U(y) - U(y_k)}{\tau}, \quad y = y_k + \tau z \right\} \\ &= \operatorname{argmin}_{y,z} \{ U(y) + \tau \Phi(z), \quad y = y_k + \tau z \} \\ &= \operatorname{argmin}_y \left\{ U(y) + \frac{1}{2\tau} \|y - y_k\|_A^2 \right\}. \end{aligned}$$

This scheme is known in literature as the De Giorgi's minimizing movement scheme [5]. This scheme exhibits unconditional stability, meaning that

$$U(y_{k+1}) + \frac{1}{2\tau} \|y_{k+1} - y_k\|_A^2 \leq U(y_k)$$

holds for any $\tau > 0$.

In this paper, we will apply the above methodology to a broad class of dissipative physical systems, which might have complicated multi-physics processes. We first show that the Onsager principle can be used to derive the evolution equations for both conserved and non-conserved unknowns. Typical examples include some celebrated nonlinear

partial differential equations (PDEs), e.g. the Allen-Cahn equation, the Cahn-Hilliard equation, Fokker-Planck equations and the Planck-Nernst-Poisson systems, etc. We also show that some relatively new thermodynamically consistent models for two phase porous media flow can also be derived in the same way. We then consider the time discretization of these significant PDEs. We consider separately the two categories of problems with conserved or nonconserved unknowns. For problems with nonconserved parameters, the time discrete scheme is similar to that for ODEs. For systems with conserved parameters, we derive novel numerical schemes, which lead to solving an optimization problem in each time step. We show that all the schemes preserve the energy dissipation structure of continuous problems. The mass conservation property is also preserved for conserved parameters. We present the applications of the method to the above mentioned PDEs. Since we focus on the time discrete schemes, the space discretization and the solution of the optimization problem can be chosen freely. For problems with nice convexity, the solution of the optimization problem can be very efficient.

The structure of the rest of paper is organized as follows. In Section 2, we present the derivation of the evolution equations by using the Onsager principle. In Section 3, we derive the time discrete schemes for two abstract problems, including many important PDEs as specific examples. In Section 4, we discuss briefly the spacial discretization and the optimization methods. We also present some numerical examples to show that our methods can indeed preserve the corresponding physical properties. Some concluding remarks are given in Section 5.

2 Onsager principle as a modeling tool

Consider a comprehensive set of variables, denoted as $\mathbf{u} = (u_1, \dots, u_s)^T$, that characterize a physical system in $\Omega \in \mathbb{R}^m$. Let $\partial_t \mathbf{u} = (\partial_t u_1, \dots, \partial_t u_s)^T$ represent the time derivative of \mathbf{u} . Assuming the system undergoes an irreversible process within a linear response regime and neglecting inertial effects, the process can be derived by using the the renowned Onsager variational principle. We demonstrate this for two distinct scenarios: one involving a system without conservation and the other for a conserved system.

2.1 Systems for nonconserved parameters

Let $\mathcal{E}(\mathbf{u})$ represent the free energy functional in a system. Its time derivative can be denoted as $\dot{\mathcal{E}}(\mathbf{u}; \partial_t \mathbf{u})$. According to the Onsager reciprocal relation, the energy dissipation function is a positive definite quadratic functional with respect to $\partial_t \mathbf{u}$ and can be expressed by $\Phi(\mathbf{u}; \partial_t \mathbf{u})$, satisfying

$$\Phi(\mathbf{u}; \lambda \mathbf{v}) = \lambda^2 \Phi(\mathbf{u}; \mathbf{v}), \quad \Phi(\mathbf{u}; \mathbf{v}) \geq 0, \quad \forall \lambda \in \mathbb{R}, \mathbf{v} : \Omega \rightarrow \mathbb{R}^s. \quad (2)$$

The Rayleighian functional is then defined as

$$\mathcal{R}(\mathbf{u}; \partial_t \mathbf{u}) := \dot{\mathcal{E}}(\mathbf{u}; \partial_t \mathbf{u}) + \Phi(\mathbf{u}; \partial_t \mathbf{u}). \quad (3)$$

By the Onsager principle, the dynamic equation of the system can be derived by minimizing the Rayleighian functional with respect to $\partial_t \mathbf{u}$, i.e.,

$$\min_{\partial_t \mathbf{u}} \mathcal{R}(\mathbf{u}; \partial_t \mathbf{u}). \quad (4)$$

It is noteworthy that $\mathcal{R}(\mathbf{u}; \partial_t \mathbf{u})$ is a quadratic positive definite form with respect to $\partial_t \mathbf{u}$ and

$$\dot{\mathcal{E}}(\mathbf{u}; \partial_t \mathbf{u}) = \left\langle \frac{\delta \mathcal{E}(\mathbf{u})}{\delta \mathbf{u}}, \partial_t \mathbf{u} \right\rangle.$$

This variational problem straightforwardly leads to the dynamic equation:

$$\frac{\delta \Phi}{\delta \partial_t \mathbf{u}} + \frac{\delta \mathcal{E}(\mathbf{u})}{\delta \mathbf{u}} = 0. \quad (5)$$

2.2 Systems for conserved parameters

In many systems, certain physical variables are conserved, such as the total mass of each component in a binary system. In such cases, we typically encounter a set of conservation equations:

$$\partial_t u_i + \nabla \cdot \mathbf{j}_i = 0, \quad i = 1, \dots, s. \quad (6)$$

Here \mathbf{j}_i represents the flux corresponding to u_i . We assume that the problem is defined in a bounded domain Ω , and $\mathbf{j}_i \cdot \mathbf{n} = 0$ on $\partial\Omega$, where \mathbf{n} is the outward unit normal vector. In such a system, the energy dissipation can be defined as a quadratic functional $\Phi(\mathbf{u}; \mathbf{j})$ with respect to $\mathbf{j} := (\mathbf{j}_1^T, \dots, \mathbf{j}_s^T)^T$. Applying the Onsager reciprocal relation, we assume that $\Phi(\mathbf{u}; \mathbf{j})$ is a positive definite quadratic form with respect to \mathbf{j} , satisfying

$$\Phi(\mathbf{u}; \lambda \mathbf{j}) = \lambda^2 \Phi(\mathbf{u}; \mathbf{j}), \quad \Phi(\mathbf{u}; \mathbf{j}) \geq 0, \quad \forall \lambda \in \mathbb{R}, \quad \mathbf{j} : \Omega \rightarrow \mathbb{R}^{ms}.$$

The Rayleighean functional is then given by

$$\mathcal{R}(\mathbf{u}; \partial_t \mathbf{u}, \mathbf{j}) := \Phi(\mathbf{u}; \mathbf{j}) + \dot{\mathcal{E}}(\mathbf{u}; \partial_t \mathbf{u}). \quad (7)$$

By the Onsager principle, the dynamics of the system can be obtained by minimizing the Rayleighean functional with respect to $(\partial_t \mathbf{u}, \mathbf{j})$ under the constraints of mass conservation equations, i.e.,

$$\begin{aligned} \min_{\partial_t \mathbf{u}, \mathbf{j}} \mathcal{R}(\mathbf{u}; \partial_t \mathbf{u}, \mathbf{j}), \\ \text{s.t. } \partial_t u_i + \nabla \cdot \mathbf{j}_i = 0, \quad i = 1, \dots, s. \end{aligned} \quad (8)$$

Once again $\dot{\mathcal{E}}(\mathbf{u}; \partial_t \mathbf{u})$ is a linear functional with respect to $\partial_t \mathbf{u}$. Introduce some multipliers μ_i , and define

$$\mathcal{R}_\mu := \mathcal{R} - \sum_{i=1}^s \int_{\Omega} \mu_i (\partial_t u_i + \nabla \cdot \mathbf{j}_i) \, dx.$$

The variational problem reduces to a dynamics equation given by the Euler-Lagrange equation of \mathcal{R}_μ ,

$$\begin{cases} \partial_t u_i + \nabla \cdot \mathbf{j}_i = 0, & i = 1, \dots, s, \\ \frac{\delta \Phi}{\delta \mathbf{j}_i} + \nabla \mu_i = 0, & i = 1, \dots, s, \\ \frac{\delta \dot{\mathcal{E}}}{\delta u_i} - \mu_i = 0, & i = 1, \dots, s. \end{cases} \quad (9)$$

In the derivation of the second equation, we have used integration by parts and the boundary condition that $\mathbf{j}_i = 0$ on $\partial\Omega$. For simplicity, we assume there are no fluxes on the boundary $\partial\Omega$ throughout the paper. Other types of boundary conditions can also be discussed, but they are more involved within the framework of the Onsager principle. We will show some examples below.

2.3 Application Examples

We present several examples widely used in science and engineering.

Example 1: The Allen-Cahn equation.

The Allen-Cahn equation (after John W. Cahn and Sam Allen) is a reaction–diffusion equation of mathematical physics which describes the phase transition of a system, characterized by an order parameter u , a scalar function defined in a domain $\Omega \subset \mathbb{R}^m$. The domain Ω represents the physical space occupied by the system.

In this context, the energy functional and the dissipation function are defined as follows:

$$\mathcal{E}(u) = \int_{\Omega} \frac{\alpha}{2} |\nabla u|^2 + F(u) \, dx + \int_{\partial\Omega} \gamma(u) \, dS, \quad (10)$$

$$\Phi(\partial_t u) = \frac{\xi_0}{2} \int_{\Omega} |\partial_t u|^2 \, dx + \frac{\xi_1}{2} \int_{\partial\Omega} |\partial_t u|^2 \, dS. \quad (11)$$

Here, α is a positive parameter, ξ_0, ξ_1 are parameters, and $F(u)$ represents the bulk free energy density, typically modeled as a double-well function, with a common choice being $F(u) = \frac{(1-u^2)^2}{4}$. The term $\gamma(u)$ denotes the free energy density on the boundary, assuming the presence of energy dissipation at the system boundary.

Direct calculations yield the following expression:

$$\begin{aligned}\dot{\mathcal{E}}(u, \partial_t u) &= \int_{\Omega} \alpha \nabla u \cdot \nabla \partial_t u + F'(u) \partial_t u \, dx + \int_{\partial\Omega} \gamma'(u) \partial_t u \, dS \\ &= \int_{\Omega} (-\alpha \Delta u + f(u)) \partial_t u \, dx + \int_{\partial\Omega} (\alpha \partial_n u + \gamma'(u)) \partial_t u \, dS.\end{aligned}$$

In the second equation, we have utilized integration by parts and introduced the notation $f(u) = F'(u)$.

The dynamic equation for the nonconserved coefficient is then reduced to:

$$\xi_0 \partial_t u - \alpha \Delta u + f(u) = 0, \quad \text{in } \Omega; \quad (12)$$

$$\xi_1 \partial_t u + \alpha \partial_n u + \gamma'(u) = 0, \quad \text{on } \partial\Omega. \quad (13)$$

When $\xi_1 = 0$, the boundary condition becomes an equilibrium condition, describing the wetting property of the boundary $\partial\Omega$ [27]. If we further assume that γ is independent of u , then the boundary condition is reduced to the standard homogeneous Neumann condition.

Example 2: The Cahn-Hilliard equation.

The Cahn-Hilliard equation (after John W. Cahn and John E. Hilliard) is an equation of mathematical physics which describes the process of phase separation in a system, characterized by an order parameter u . The free energy functional is identical to that of the Allen-Cahn equation in Equ. (10). However, in this case, the parameter u is conserved and satisfies

$$\partial_t u + \nabla \cdot \mathbf{j} = 0, \quad \text{in } \Omega, \quad \mathbf{j} \cdot \mathbf{n}|_{\partial\Omega} = 0,$$

where $\mathbf{j} : \Omega \rightarrow \mathbb{R}^m$ is a vector function. In this scenario, the dissipation functional is defined as

$$\Phi = \int_{\Omega} \frac{\mathbf{j}^T A(u) \mathbf{j}}{2} \, dx + \frac{\xi}{2} \int_{\partial\Omega} |\partial_t u|^2 \, dS,$$

where $A(u)$ is a positive definite symmetric matrix function, akin to a friction coefficient. The dynamic equation for the conserved parameter is then reduced to

$$\begin{aligned}\partial_t u + \nabla \cdot \mathbf{j} &= 0, & \text{in } \Omega, \\ A(u) \mathbf{j} &= -\nabla \mu, & \text{in } \Omega, \\ \mu &= -\alpha \Delta u + f(u), & \text{in } \Omega, \\ \mathbf{j} \cdot \mathbf{n} &= 0 & \text{on } \partial\Omega, \\ \xi \partial_t u &= -(\partial_n u + \gamma'(u)) & \text{on } \partial\Omega.\end{aligned}$$

Introduce a mobility matrix $M(u) = A^{-1}$, we obtain

$$\partial_t u = \nabla \cdot (M(u) \nabla \mu), \quad \text{in } \Omega, \quad (14)$$

$$\mu = -\alpha \Delta u + f(u), \quad \text{in } \Omega, \quad (15)$$

$$M(u) \nabla \mu \cdot \mathbf{n} = 0, \quad \text{on } \partial\Omega, \quad (16)$$

$$\xi \partial_t u = -(\partial_n u + \gamma'(u)), \quad \text{on } \partial\Omega. \quad (17)$$

This represents a general form of the Cahn-Hilliard equation, which has been used to describe wetting phenomena of a droplet in [3]. Once again, when $\xi = 0$, we obtain the equilibrium boundary condition for u on $\partial\Omega$.

Example 3: The Fokker-Planck equation.

In statistical mechanics and information theory, the Fokker-Planck equation (FPE) (after Adriaan Fokker and Max Planck in 1914 and 1917) is used to investigate the diffusion of a specific type of particles under the influence of an external potential field. This equation can also be extended to other observables [18]. Here we are concerned with FPE having the form

$$\partial_t u = \nabla \cdot (\nabla U u) + \beta^{-1} \Delta u,$$

where $u > 0$ represents the density function of the particles, $U(x)$ represents an external potential field, and $\beta > 0$ is a given constant. It is known [17] the FPE dynamics can be regarded as a gradient flow of the free energy of form

$$\mathcal{E}(u) = \beta^{-1} \int_{\Omega} u \log u + uU(x) dx,$$

with respect to the Wasserstein metric on an appropriate class of probability measures. It is also well-known that the Fokker-Planck equation is inherently related to the Itô stochastic differential equation [33]

$$dX(t) = -\nabla U(X(t))dt + \sqrt{2\beta^{-1}}dW(t), \quad X(0) = X^0.$$

Here, $W(t)$ is a standard d -dimensional Wiener process, and X^0 is an d -dimensional random vector with probability density $u(t=0)$. In this context, u furnishes the probability density at time t for finding the particle at position $x \in \Omega$.

Here we demonstrate how to derive FPE by the Onsager principle. Considering the conservation property:

$$\partial_t u + \nabla \cdot \mathbf{j} = 0, \quad \text{in } \Omega, \quad \mathbf{j} \cdot \mathbf{n}|_{\partial\Omega} = 0,$$

where \mathbf{j} is the mass flux, we define the energy dissipation function as

$$\Phi = \frac{1}{2} \int_{\Omega} \frac{|\mathbf{j}|^2}{u} dx.$$

By direct calculation, the chemical potential in this case is given by

$$\mu = \frac{\delta \mathcal{E}}{\delta u} = \beta^{-1}(1 + \log u) + U.$$

Then by applying the Onsager principle,

$$\begin{aligned} \min_{\partial_t u, \mathbf{j}} \mathcal{R} &= \Phi + \dot{\mathcal{E}}, \\ \text{s.t. } \partial_t u + \nabla \cdot \mathbf{j} &= 0 \text{ in } \Omega, \quad \mathbf{j} \cdot \mathbf{n}|_{\partial\Omega} = 0, \end{aligned}$$

the dynamic equation for conserved system is reduced to

$$\begin{aligned} \partial_t u + \nabla \cdot \mathbf{j} &= 0, & \text{in } \Omega, \\ \frac{\mathbf{j}}{u} + \nabla \mu &= 0, & \text{in } \Omega, \\ \mu &= \beta^{-1}(1 + \log u) + U, & \text{in } \Omega, \\ \partial_n \mu &= 0 & \text{on } \partial\Omega. \end{aligned}$$

We can do further simplification by substituting the third equation into the second one. This leads to

$$\partial_t u + \nabla \cdot \mathbf{j} = 0, \quad \text{in } \Omega, \tag{18}$$

$$\mathbf{j} = -(\beta^{-1} \nabla u + u \nabla U), \quad \text{in } \Omega, \tag{19}$$

$$\mathbf{j} \cdot \mathbf{n} = 0 \quad \text{on } \partial\Omega. \tag{20}$$

Example 4: The Planck-Nernst-Poisson equation.

The Nernst–Planck equation, named after Walther Nernst and Max Planck, is a conservation of mass equation employed to depict the movement of a charged chemical species in a fluid medium. It extends Fick’s law of diffusion to account for cases where the diffusing particles are also influenced by electrostatic forces, as governed by the Poisson equation. The Planck-Nernst-Poisson (PNP) equation specifically describes the diffusion of ions in solutions. It is crucial to consider the energy associated with the static electric field.

Suppose there are s types of ions, and the density of particles is characterized by u_i for $i = 1, \dots, s$. These density functions satisfy the conservation equation:

$$\partial_t u_i + \nabla \cdot \mathbf{j}_i = 0 \text{ in } \Omega, \quad i = 1, \dots, s; \quad \mathbf{j}_i \cdot \mathbf{n} = 0 \quad \text{on } \partial\Omega.$$

The total free energy is given by

$$\mathcal{E}(\mathbf{u}) = \int_{\Omega} \sum_{i=1}^s u_i \log u_i + \frac{\varepsilon_0}{2} |\nabla \varphi(x)|^2 \, dx,$$

where φ is the electric potential, $\varepsilon_0(x)$ is the permittivity. It is related to u_i by the static electric field equation:

$$-\nabla \cdot (\varepsilon_0 \nabla \varphi) = f(x) + \sum_{i=1}^n z_i u_i, \text{ in } \Omega, \quad (21)$$

where z_i is the rescaled charge, $f(x)$ is the permanent (fixed) charge density of the system. Boundary conditions for φ can vary, we simply take $\partial_n \varphi$ on $\partial\Omega$. The energy dissipation functions is defined as,

$$\Phi := \frac{1}{2} \int_{\Omega} \sum_i D_i^{-1}(x) u_i^{-1} |\mathbf{j}_i|^2 \, dx,$$

where $D_i(x) > 0$ is an diffusion coefficient for i -th ion. Direct calculations show that

$$\frac{\delta \mathcal{E}}{\delta u_i} = (1 + \log u_i + z_i \varphi),$$

where we have used the static electric field equation and the boundary condition $\partial_n \varphi = 0$. Then by applying the Onsager principle,

$$\min_{\partial_t \mathbf{u}, \mathbf{j}} \mathcal{R} = \frac{1}{2} \int_{\Omega} \sum_i D_i^{-1}(x) u_i^{-1} |\mathbf{j}_i|^2 \, dx + \dot{\mathcal{E}},$$

$$s.t. \quad \partial_t u_i + \nabla \cdot \mathbf{j}_i = 0 \text{ in } \Omega, \quad \mathbf{j}_i \cdot \mathbf{n}|_{\partial\Omega} = 0,$$

we obtain the PNP system of equations:

$$\partial_t u_i = \nabla \cdot [D_i(x)(\nabla u_i + z_i u_i \nabla \varphi)], \quad x \in \Omega, \quad i = 1, \dots, s; \quad (22)$$

$$-\nabla \cdot (\varepsilon_0 \nabla \varphi) = f(x) + \sum_{i=1}^s z_i u_i, \quad x \in \Omega, \quad (23)$$

$$\partial_n \varphi = 0 \quad \text{on } \partial\Omega. \quad (24)$$

Note that the external electrostatic potential φ is influenced by applied potential, which can be modeled by prescribing a boundary condition. The analysis above applies well to a general form of boundary conditions:

$$\alpha \varphi + \beta \varepsilon_0(x) \partial_n \varphi = 0, \quad x \in \partial\Omega,$$

if we take a modified energy of form

$$\mathcal{E}(\mathbf{u}) = \int_{\Omega} \left(\sum_{i=1}^s u_i \log u_i + \frac{1}{2} (f + \sum_{i=1}^s z_i u_i) \varphi(x) \right) \, dx.$$

Here α, β are physical parameters such that $\alpha \cdot \beta \geq 0$. Refer to [22] for cases with non-homogeneous boundary conditions.

Example 5: The Maxwell-Stefan diffusion equation.

For a system containing multiple types of particles, the Maxwell-Stefan diffusion equation is employed to describe the diffusion of the multi-component system. The equations that describe these transport processes have been developed independently and in parallel by James Clerk Maxwell (1965) for dilute gases and Josef Stefan (1871) for liquids. Let $u_i > 0, i = 1, \dots, s$ denote the number density of each component, and all components are conserved, satisfying the conservation equation

$$\partial_t u_i + \nabla \cdot \mathbf{j}_i = 0 \text{ in } \Omega, \quad j = 1, \dots, s, \quad \mathbf{j}_i \cdot \mathbf{n}|_{\partial\Omega} = 0. \quad (25)$$

Here, \mathbf{j}_i is the flux for the i -th component. The total number density of all components is assumed to be constant:

$$\sum_{i=1}^s u_i = 1. \quad (26)$$

The free energy in the system is given by

$$\mathcal{E}(\mathbf{u}) = \int_{\Omega} \sum_{i=1}^s u_i \log u_i \, dx, \quad (27)$$

and the dissipation function is defined as

$$\Phi(\mathbf{u}; \mathbf{j}) = \frac{1}{4} \int_{\Omega} \sum_{i,j=1}^s b_{ij} u_i u_j \left| \frac{\mathbf{j}_i}{u_i} - \frac{\mathbf{j}_j}{u_j} \right|^2 \, dx. \quad (28)$$

Here coefficient $B = (b_{ij})$ is symmetric and positive definite.

To simplify the derivation, we introduce new variables $\mathbf{v}_i = \frac{\mathbf{j}_i}{u_i}$ to replace \mathbf{j}_i . In this case, the dissipation function in Equ. (28) is rewritten as

$$\Phi(\mathbf{u}; \mathbf{v}) = \frac{1}{4} \int_{\Omega} \sum_{i,j=1}^s b_{ij} u_i u_j |\mathbf{v}_i - \mathbf{v}_j|^2 \, dx.$$

The mass conservation equation (25) is reduced to

$$\partial_t u_i + \nabla \cdot (u_i \mathbf{v}_i) = 0 \text{ in } \Omega, \quad j = 1, \dots, s; \quad \mathbf{u} \cdot \mathbf{n}|_{\partial\Omega} = 0.$$

The additional constraint in Equ. (26) is equivalent to the equation

$$\sum_{i=1}^s \nabla \cdot (u_i \mathbf{v}_i) = 0.$$

Applying the Onsager variational principle, direct calculations lead to

$$\dot{\mathcal{E}}(\mathbf{u}; \partial_t \mathbf{u}) = \int_{\Omega} \sum_{i=1}^s (1 + \log u_i) \partial_t u_i \, dx.$$

Then the Rayleighian is defined as

$$\mathcal{R}(\mathbf{u}; \partial_t \mathbf{u}, \mathbf{v}) = \frac{1}{4} \int_{\Omega} \sum_{i,j=1}^s b_{ij} u_i u_j |\mathbf{v}_i - \mathbf{v}_j|^2 \, dx + \int_{\Omega} \sum_{i=1}^s (1 + \log u_i) \partial_t u_i \, dx.$$

The dynamic equation is derived by minimizing the Rayleighian functional:

$$\begin{aligned} \min_{\mathbf{u}, \mathbf{v}} \mathcal{R}(\mathbf{u}; \partial_t \mathbf{u}, \mathbf{v}), \\ \text{s.t. } \partial_t u_i + \nabla \cdot (u_i \mathbf{v}_i) = 0, \quad j = 1, \dots, s, \\ \sum_{i=1}^s \nabla \cdot (u_i \mathbf{v}_i) = 0. \end{aligned}$$

Introducing Lagrangian multipliers μ_i for the conservation equation and a multiplier p for the last equation, we set

$$\mathcal{R}_\mu(\mathbf{u}; \partial_t \mathbf{u}, \mathbf{v}) := \mathcal{R}(\mathbf{u}; \partial_t \mathbf{u}, \mathbf{v}) - \sum_{i=1}^s \int_{\Omega} \mu_i (\partial_t u_i + \nabla \cdot (u_i \mathbf{v}_i)) \, dx - \int_{\Omega} p \left(\sum_{i=1}^s \nabla \cdot (u_i \mathbf{v}_i) \right) \, dx.$$

Considering the first order derivation of the functional, we obtain the system:

$$\partial_t u_i + \nabla \cdot (u_i \mathbf{v}_i) = 0, \quad \text{in } \Omega, \quad (29)$$

$$\sum_{j=1}^s b_{ij} u_j (\mathbf{v}_i - \mathbf{v}_j) + \nabla \mu_i = -\nabla p, \quad \text{in } \Omega, \quad (30)$$

$$\mu_i = 1 + \log u_i \quad \text{in } \Omega, \quad (31)$$

$$\sum_{i=1}^s \nabla \cdot (u_i \mathbf{v}_i) = 0, \quad \text{in } \Omega, \quad (32)$$

where we have used the boundary conditions $\partial_n \mu_i = 0$ and $\partial_n p = 0$. Substitute the third equation into the second one, we get

$$\sum_{j=1}^s b_{ij} u_j (\mathbf{v}_i - \mathbf{v}_j) + \frac{1}{u_i} \nabla u_i = -\nabla p.$$

By the symmetricity of b_{ij} , we have $\sum_{j=1}^s b_{ij} u_i u_j (\mathbf{v}_i - \mathbf{v}_j) = 0$. Thus by multiplying the above equation with u_i and do summation with respect to i , we obtain

$$-\nabla p = \frac{1}{\sum_{i=1}^s u_i} \sum_{i=1}^s \nabla u_i.$$

The system (29)-(32) is further simplified to

$$\begin{aligned} \partial_t u_i + \nabla \cdot (u_i \mathbf{v}_i) &= 0, \quad \text{in } \Omega, \\ \sum_{j=1}^s b_{ij} u_j (\mathbf{v}_i - \mathbf{v}_j) + \frac{1}{u_i} \nabla u_i &= \frac{1}{\sum_{j=1}^s u_j} \sum_{j=1}^s \nabla u_j, \quad \text{in } \Omega. \end{aligned}$$

Note that the boundary conditions are reduced to $\partial_n u_i = 0$ on $\partial\Omega$. The system above can be expressed as

$$\partial_t u_i + \nabla \cdot (u_i \mathbf{v}_i) = 0, \quad \text{in } \Omega, \quad (33)$$

$$\sum_{j=1}^s b_{ij} u_j (\mathbf{v}_i - \mathbf{v}_j) + \nabla \log u_i = \frac{1}{\sum_{j=1}^s u_j} \sum_{j=1}^s u_j \nabla \log u_j, \quad \text{in } \Omega, \quad (34)$$

$$\partial_n u_i = 0 \quad \text{on } \partial\Omega. \quad (35)$$

Example 6: The incompressible and immiscible multi-phase flow in porous media.

We now turn our attention to the incompressible and immiscible multi-phase flow in porous media which has extensive applications in hydrology and petroleum reservoir engineerings. Recently, a thermodynamically consistent model was developed for the incompressible and immiscible two-phase flow in porous media [12]. Different from the classical models for two-phase flow in porous media, the model introduces a logarithmic free energy to characterize

the capillarity effect, and the system satisfies the energy dissipation law. In the following, we can also rebuild the thermodynamically consistent model for the incompressible and immiscible multi-phase flow in porous media based on the Onsager principle.

Let $u_i, i = 1, \dots, s$, represent the volume fraction of the i -th phase which is also known as saturation, ensuring that $\sum_{i=1}^s u_i = 1$. Let ϕ be porosity of the porous media. The unknown function satisfies the following conservation law:

$$\phi \partial_t u_i + \nabla \cdot \mathbf{v}_i = 0, \quad i = 1, \dots, s, \quad \mathbf{v}_i \cdot \mathbf{n}|_{\partial\Omega} = 0.$$

Here, \mathbf{v}_i denotes the average velocity of the i -th phase fluid. In some cases, assuming that the equilibrium state is determined by a free energy $\mathcal{E}(\mathbf{u}) = \int_{\Omega} \phi F(\mathbf{u}) dx$ is convenient. One possible choice for $F(\mathbf{u})$ is

$$F(\mathbf{u}) = \sum_{j=1}^s \sigma_j u_j (\log u_j - 1) + \sum_{i,j=1}^s \alpha_{ij} u_i u_j + \sum_{j=1}^s b_j u_j.$$

The energy dissipation in this case is given by

$$\Phi = \int_{\Omega} \sum_{i=1}^s \frac{1}{2} \mathbf{v}_i K_i^{-1} \mathbf{v}_i dx.$$

Here, K_i is a positive definite and symmetric matrix which is dependent of \mathbf{u} . Similar to the derivation for the Maxwell-Stefan equation, we obtain

$$\phi \partial_t u_i + \nabla \cdot \mathbf{v}_i = 0, \quad i = 1, \dots, s, \quad \text{in } \Omega, \quad (36)$$

$$\mathbf{v}_i = -K_i (\nabla \mu_i + \nabla p), \quad i = 1, \dots, s, \quad \text{in } \Omega, \quad (37)$$

$$\mu_i = \frac{\partial F}{\partial u_i}, \quad i = 1, \dots, s, \quad \text{in } \Omega, \quad (38)$$

$$\sum_{i=1}^s u_i = 1, \quad \text{in } \Omega, \quad (39)$$

$$\partial_n \mu_i + \partial_n p = 0, \quad \text{on } \partial\Omega. \quad (40)$$

Example 7: The multi-phase flow in porous media with rock compressibility.

For the multi-phase flow in porous media with rock compressibility, the variation of porosity with respect to effective pressure can be expressed as

$$\frac{d\phi}{\phi} = \gamma dp_e, \quad (41)$$

which yields

$$\phi = \phi_r e^{\gamma(p_e - p_r)}. \quad (42)$$

Here γ is the rock compressibility coefficient, p_r is the reference or initial pressure and ϕ_r is the porosity at the reference pressure. The absolute permeability K of the porous media changes with the porosity according to the Kozeny-Carman equation:

$$K = K_0 \frac{\phi^3 (1 - \phi_r)^2}{\phi_r^3 (1 - \phi)^2}, \quad (43)$$

where K_0 is the initial intrinsic permeability. The rock compressibility caused by the pore fluid pressure has been recognized as an important factor influencing many subsurface processes which include the oil/gas production and the geological stability. For the modeling of the changes of rock properties, one approach is to use the Biot-type model for the rock, and another one is the rock compressibility model as (41). A thermodynamically consistent

model for the incompressible and immiscible two-phase flow in porous media with rock compressibility was developed in [19]. We can rebuild the thermodynamically consistent model for the multi-phase case by the Onsager principle in the following.

Now, let's introduce the rock free energy denoted by R . We assume that the work done by the effective pore fluid pressure exerted on rocks is transferred to the rock free energy. The variation of rock free energy with respect to effective pressure is described as:

$$dR = p_e d\phi.$$

The total free energy is given by

$$\mathcal{E}(\mathbf{u}, \phi) = \int_{\Omega} \phi F(\mathbf{u}) dx + \int_{\Omega} R dx,$$

where $F(\mathbf{u})$ is given as Example 6. The time derivative of the energy, $\dot{\mathcal{E}}(\mathbf{u}; \partial_t \mathbf{u}, \phi; \partial_t \phi)$, is expressed as

$$\dot{\mathcal{E}}(\mathbf{u}; \partial_t \mathbf{u}, \phi; \partial_t \phi) = \int_{\Omega} \partial_t(\phi F(\mathbf{u})) dx + \int_{\Omega} p_e \partial_t \phi dx.$$

The energy dissipation is similar to that in Example 6.

The unknown functions satisfy the conservation laws:

$$\partial_t(\phi u_i) + \nabla \cdot \mathbf{v}_i = 0, \quad i = 1, \dots, s.$$

The saturation of each phase satisfies the saturation constraint $\sum_{i=1}^s u_i = 1$. By the conservation law, we also have

$$\sum_{i=1}^s u_i \partial_t \phi + \sum_{i=1}^s \nabla \cdot \mathbf{v}_i = 0.$$

If the above equation holds true, we can directly obtain the saturation constraint $\sum_{i=1}^s u_i = 1$ by the conservation law and the initial saturation constraint $\sum_{i=1}^s u_i(0, x) = 1$.

The dynamic equation can be derived by minimizing the Rayleighian functional as follows:

$$\begin{aligned} \min_{\partial_t \mathbf{u}, \partial_t \phi, \mathbf{v}} \quad & \mathcal{R}(\mathbf{u}; \partial_t \mathbf{u}, \phi; \partial_t \phi, \mathbf{v}) \\ \text{s.t.} \quad & \partial_t(\phi u_i) + \nabla \cdot \mathbf{v}_i = 0, \quad i = 1, \dots, s, \\ & \sum_{i=1}^s u_i \partial_t \phi + \sum_{i=1}^s \nabla \cdot \mathbf{v}_i = 0. \end{aligned}$$

Introducing $\mu = (\mu_1, \dots, \mu_s)$ and p as the Lagrangian multipliers, we set

$$\begin{aligned} \mathcal{R}_L(\mathbf{u}; \partial_t \mathbf{u}, \phi; \partial_t \phi, \mathbf{v}, \mu, p) &= \mathcal{R}(\mathbf{u}; \partial_t \mathbf{u}, \phi; \partial_t \phi, \mathbf{v}) - \sum_{i=1}^s \int_{\Omega} \mu_i (\partial_t(\phi u_i) + \nabla \cdot \mathbf{v}_i) dx \\ &\quad - \int_{\Omega} p \left(\sum_{i=1}^s u_i \partial_t \phi + \sum_{i=1}^s \nabla \cdot \mathbf{v}_i \right) dx. \end{aligned}$$

By the Euler-Lagrange equation, (42) and (43), we have

$$\partial_t(\phi u_i) + \nabla \cdot \mathbf{v}_i = 0, \quad i = 1, \dots, s, \quad \text{in } \Omega, \quad (44)$$

$$\mathbf{v}_i = -K_i(\nabla \mu_i + \nabla p), \quad i = 1, \dots, s, \quad \text{in } \Omega, \quad (45)$$

$$\mu_i = \frac{\partial F}{\partial u_i}, \quad i = 1, \dots, s, \quad \text{in } \Omega, \quad (46)$$

$$\sum_{i=1}^s u_i = 1, \quad \text{in } \Omega, \quad (47)$$

$$p_e = p + \sum_{i=1}^s u_i \mu_i - F(\mathbf{u}), \quad \text{in } \Omega, \quad (48)$$

$$\phi = \phi_r e^{\gamma(p_e - p_r)}, \quad \text{in } \Omega, \quad (49)$$

$$K = K_0 \frac{\phi^3 (1 - \phi_r)^2}{\phi_r^3 (1 - \phi)^2}, \quad \text{in } \Omega. \quad (50)$$

Here $K_i = \lambda_i K$, and $\lambda_i = \frac{k_{ri}(\mathbf{u})}{\eta_i}$, where k_{ri} and η_i are the relative permeability and viscosity of the phase i .

3 Time-discretization based on the Onsager principle

In this section, we present the time discretization of partial differential equations using the Onsager principle. We first introduce the main idea for the abstract problems and then apply them to some typical examples.

We discretize the time interval $[0, T]$ by considering $0 = t_0 < t_1 < \dots < t_N = T$. Suppose that we already computed the solution at time t_k . We will compute \mathbf{u}^{k+1} by employing a discrete version of the Onsager principle.

3.1 Discretization for systems with nonconserved parameters

Suppose \mathbf{u}^k is known with a time step $\tau = t_{k+1} - t_k$. We discretize the Rayleighian functional as follows,

$$\mathcal{R}_\tau^k(\mathbf{u}^k; \mathbf{u}) := D_\tau \mathcal{E}(\mathbf{u}^k; \mathbf{u}) + \Phi_\tau^k(\mathbf{u}, D_\tau \mathbf{u}^k), \quad (51)$$

where

$$\Phi_\tau^k(\mathbf{u}, D_\tau \mathbf{u}^k) := \Phi\left(\mathbf{u}; \frac{\mathbf{u} - \mathbf{u}^k}{\tau}\right), \quad (52)$$

$$D_\tau \mathcal{E}(\mathbf{u}^k; \mathbf{u}) := \frac{\mathcal{E}(\mathbf{u}) - \mathcal{E}(\mathbf{u}^k)}{\tau}. \quad (53)$$

Then the unknowns \mathbf{u}^{k+1} at time t_{k+1} are computed by solving the minimization problem,

$$\mathbf{u}^{k+1} = \operatorname{argmin}_{\mathbf{u}} \mathcal{R}_\tau^k(\mathbf{u}^k; \mathbf{u}).$$

Or equivalently,

$$\mathbf{u}^{k+1} = \operatorname{argmin}_{\mathbf{u}} \mathcal{E}(\mathbf{u}) + \frac{1}{\tau} \Phi(\mathbf{u}; \mathbf{u} - \mathbf{u}^k). \quad (54)$$

Here we have used the fact that $\Phi(\mathbf{u}; \partial_t \mathbf{u})$ is a positive definite quadratic form of $\partial_t \mathbf{u}$. We can see that \mathbf{u}^{k+1} can be seen as a generalized minimizing movement solution. It is also referred to as a JKO scheme in the literature [17].

The scheme is unconditionally stable by definition. The following proposition is easy to verify. Denoted by J_τ the set of minimizers of the above problem (54).

Proposition 1 *When J_τ is not empty, for any choice $\mathbf{u}^{k+1} \in J_\tau$, we have that*

$$\mathcal{E}(\mathbf{u}^{k+1}) \leq \mathcal{E}(\mathbf{u}^k) - \frac{1}{\tau} \Phi(\mathbf{u}^{k+1}, \mathbf{u}^{k+1} - \mathbf{u}^k) \leq \mathcal{E}(\mathbf{u}^k).$$

Proof By definition, we have

$$\mathcal{E}(\mathbf{u}^{k+1}) + \frac{1}{\tau} \Phi(\mathbf{u}^{k+1}; \mathbf{u}^{k+1} - \mathbf{u}^k) \leq \mathcal{E}(\mathbf{u}^k) + \frac{1}{\tau} \Phi(\mathbf{u}^k; \mathbf{0}) = \mathcal{E}(\mathbf{u}^k).$$

Here we have used the fact that $\Phi(\mathbf{u}; \mathbf{j})$ is a positive definite quadratic form with respect to \mathbf{j} .

□

3.2 Discretization for systems with conserved parameters

When the parameters in a physical system are conserved, we can discretize the system similarly. Suppose, again, that \mathbf{u}^k is already known and we will compute \mathbf{u}^{k+1} by using the discrete Onsager principle. We first discretize the conservation equations as follows:

$$\frac{u_i - u_i^k}{\tau} + \nabla \cdot \mathbf{j}_i = 0, \quad (55)$$

where \mathbf{j}_i is independent of time and satisfies $\mathbf{j}_i \cdot \mathbf{n} = 0$ on $\partial\Omega$. Then, the energy functional and the dissipation function are discretized as follows:

$$\begin{aligned} \Phi_\tau^k(\mathbf{u}, \mathbf{j}) &:= \Phi(\mathbf{u}; \mathbf{j}), \\ D_\tau \mathcal{E}(\mathbf{u}^k; \mathbf{u}) &:= \frac{\mathcal{E}(\mathbf{u}) - \mathcal{E}(\mathbf{u}^k)}{\tau}. \end{aligned}$$

The \mathbf{u}^{k+1} and \mathbf{j}^{k+1} are obtained by minimizing the discrete Rayleighian functional as follows,

$$\begin{aligned} (\mathbf{u}^{k+1}, \mathbf{j}^{k+1}) = \operatorname{argmin}_{\mathbf{u}, \mathbf{j}} \mathcal{R}_\tau^k(\mathbf{u}, \mathbf{j}) &:= \Phi_\tau^k(\mathbf{u}, \mathbf{j}) + D_\tau \mathcal{E}(\mathbf{u}^k; \mathbf{u}) \\ \text{s.t.} \quad \frac{u_i - u_i^k}{\tau} + \nabla \cdot \mathbf{j}_i &= 0, \quad i = 1, \dots, s. \end{aligned} \quad (56)$$

By introduce a variable $\mathbf{m} = \tau \mathbf{j}$, the problem is equivalent to

$$\begin{aligned} (\mathbf{u}^{k+1}, \mathbf{m}^{k+1}) = \operatorname{argmin}_{\mathbf{u}, \mathbf{m}} \mathcal{E}(\mathbf{u}) + \frac{1}{\tau} \Phi_\tau^k(\mathbf{u}, \mathbf{m}), \\ \text{s.t.} \quad u_i - u_i^k + \nabla \cdot \mathbf{m}_i &= 0. \end{aligned} \quad (57)$$

Here we again used the fact that $\Phi(\mathbf{u}; \mathbf{j})$ is a quadratic form with respect to \mathbf{j} .

Proposition 2 *Suppose $(\mathbf{u}^{k+1}, \mathbf{m}^{k+1})$ is a minimizer of the minimizing problem (57), we then have*

$$\mathcal{E}(\mathbf{u}^{k+1}) \leq \mathcal{E}(\mathbf{u}^k) - \frac{1}{\tau} \Phi(\mathbf{u}^{k+1}; \mathbf{m}^{k+1}) \leq \mathcal{E}(\mathbf{u}^k),$$

and \mathbf{u}^{k+1} satisfies the mass conservation equation that

$$\int_{\Omega} u_i^{k+1} \, dx = \int_{\Omega} u_i^k \, dx, \quad i = 1, \dots, s.$$

Proof The proof of the energy inequality is similar to that in Proposition 1. By definition, we have

$$\mathcal{E}(\mathbf{u}^{k+1}) + \frac{1}{\tau} \Phi(\mathbf{u}^{k+1}; \mathbf{m}^{k+1}) \leq \mathcal{E}(\mathbf{u}^k) + \frac{1}{\tau} \Phi(\mathbf{u}^k; \mathbf{0}) = \mathcal{E}(\mathbf{u}^k).$$

Here we have used the fact that $\Phi(\mathbf{u}; \mathbf{j})$ is a positive definite quadratic form with respect to \mathbf{j} . The mass conservation equation is obtained by integrate the constraint

$$\int_{\Omega} u_i^{k+1} \, dx = \int_{\Omega} u_i^k \, dx + \int_{\Omega} \nabla \cdot \mathbf{m}^{k+1} \, dx = \int_{\Omega} u_i^k \, dx + \int_{\partial\Omega} \mathbf{m}^{k+1} \cdot \mathbf{n} \, dx = \int_{\Omega} u_i^k \, dx,$$

where we have used the assumption that $\mathbf{m}^{k+1} \cdot \mathbf{n} = \tau \mathbf{j}^{k+1} \cdot \mathbf{n} = 0$.

□

Remark 1 *Notice that we derive the abstract discrete schemes under the no flux boundary condition. For more general conditions, we can also derive the corresponding schemes in a similar approach. For example, if we consider periodic conditions, all the above derivations are same as that for no flux boundary conditions.*

3.3 Time discretization by examples

Example 1: The Allen-Cahn equation.

Consider the Allen-Cahn equation described in Example 1 of Section 2.3, we apply the Onsager principle to obtain the following time discretization:

$$\mathbf{u}^{k+1} = \operatorname{argmin}_{u \in H^1(\Omega)} \left\{ \mathcal{E}(u) + \frac{1}{\tau} \Phi(u - u^k) \right\},$$

where

$$\begin{aligned} \mathcal{E}(u) &= \int_{\Omega} \frac{\alpha}{2} |\nabla u|^2 + F(u) \, dx + \int_{\partial\Omega} \gamma(u) \, dS, \\ \Phi(v) &= \frac{1}{2} \int_{\Omega} |v|^2 \, dx + \frac{\xi_1}{2} \int_{\partial\Omega} |v|^2 \, dS. \end{aligned}$$

This is a constraint minimization problem. When τ is small, the minimizing problem may have a unique minimizer, which can be obtained by the backward Euler scheme:

$$\begin{aligned} \frac{u^{k+1} - u^k}{\tau} &= \alpha \Delta u^{k+1} - F'(u^{k+1}) \quad \text{in } \Omega, \\ \xi_1 \frac{u^{k+1} - u^k}{\tau} + \alpha \partial_n u^{k+1} + \gamma'(u^{k+1}) &= 0 \quad \text{on } \partial\Omega. \end{aligned}$$

In a simple setting with $\gamma(u) = \text{const}$, $\xi_1 = 0$, and subject to periodic boundary conditions, we are let to

$$u^{k+1} = \operatorname{argmin}_{u \in H^1(\Omega)} \int_{\Omega} \frac{(u - u^k)^2}{2\tau} + \frac{\alpha}{2} |\nabla u|^2 + F(u) \, dx.$$

If $F(u) = \frac{(1-u^2)^2}{4}$, we have $f(u) = F'(u) = u^3 - u$.

Example 2: The Cahn-Hilliard equation.

Consider the Cahn-Hilliard equation described in Example 2 of Section 2.3, we introduce a space

$$\mathbf{V} := \{ \mathbf{v} : \Omega \rightarrow \mathbb{R}^m : \mathbf{v} \in H(\operatorname{div}, \Omega), \mathbf{v} \cdot \mathbf{n} = 0 \text{ on } \partial\Omega \}.$$

According to the Onsager principle, we obtain our time-discrete variational formulation of the Cahn-Hilliard equation: $(u^{k+1}, \mathbf{j}^{k+1})$ is obtained by solving the following constraint optimization problem:

$$\begin{aligned} \min_{u \in H^1(\Omega), \mathbf{j} \in \mathbf{V}} & \left\{ \frac{\tau}{2} \int_{\Omega} \mathbf{j}^\top M^{-1}(u) \mathbf{j} \, dx + \frac{\xi}{2\tau} \int_{\partial\Omega} |u - u^k|^2 \, dS + \int_{\Omega} \frac{\alpha}{2} |\nabla u|^2 + F(u) \, dx + \int_{\partial\Omega} \gamma(u) \, dS \right\}, \\ \text{s.t.} & \quad \frac{u - u^k}{\tau} + \nabla \cdot \mathbf{j} = 0 \text{ in } \Omega. \end{aligned}$$

Here τ is the time step, with initial data u^0 . When τ is small and u has good regularity, the minimizer of the problem may be unique and satisfies the Euler-Lagrange equation.

$$\begin{aligned} \frac{u - u^k}{\tau} &= \nabla \cdot (M(u) \nabla \mu), \quad \text{in } \Omega, \\ \mu &= \alpha \Delta u - F'(u), \quad \text{in } \Omega, \\ M(u) \nabla \mu \cdot \mathbf{n} &= 0, \quad \text{on } \partial\Omega, \\ \xi \frac{u - u^k}{\tau} &= -(\partial_n u + \gamma'(u)), \quad \text{on } \partial\Omega. \end{aligned}$$

This is an implicit time discretization of the Cahn-Hilliard equation.

Example 3: The Fokker-Planck equation.

For the Fokker-Planck equation, the scheme (57) is reduced to

$$\begin{aligned}
(u^{k+1}, \mathbf{m}^{k+1}) &= \operatorname{argmin}_{u \in L^1_+(\Omega), \mathbf{m} \in \mathbf{V}} \left\{ \frac{1}{2\tau} \int_{\Omega} \frac{|\mathbf{m}|^2}{u} \, dx + \int_{\Omega} \beta^{-1} u \log u + uU(x) \, dx \right\}, \\
&\quad \text{s.t. } u - u^k + \nabla \cdot \mathbf{m} = 0.
\end{aligned}$$

Under appropriate conditions on U , one can verify that the underlying functional is convex with linear constraints so that there exists a unique minimizer. We could also prove that $u^{k+1} > 0$, i.e. the scheme is positive preserving. This discrete formulation serves as a natural approximation to the celebrated Jordan–Kinderlehrer–Otto (JKO) scheme:

$$\text{Determine } u^{k+1} \text{ that minimizes } \left\{ \frac{1}{2\tau} W_2^2(u, u^k) + \int_{\Omega} \beta^{-1} u \log u + uU(x) \, dx \right\},$$

where W_2 is the 2-Wasserstein distance [17]. That is

$$W^2(a, b) \sim \inf_{m \in \mathbf{V}} \left\{ \int_{\Omega} \frac{|m|^2}{a} \, dx, \quad b - a + \nabla \cdot m = 0 \right\}.$$

In fact, such an approximation is even more clear when comparing with

$$W^2(a, b) = \inf_{m, \rho} \left\{ \int_0^1 \int_{\Omega} \rho |v|^2 \, dx \, ds, \quad \partial_s \rho + \nabla \cdot (\rho v) = 0, \quad \rho(0) = a, \quad \rho(1) = b \right\}.$$

This, called the Benamou–Brenier formula [1], establishes a tight connection between absolutely continuous curves in the probability density space with Wasserstein metric and solutions to the continuity equation.

Example 4: The Plank-Nernst-Poisson equations.

For the Plank-Nernst-Poisson, we have

$$\begin{aligned}
(\mathbf{u}^{k+1}, \mathbf{m}^{k+1}) &= \operatorname{argmin}_{\mathbf{u} \in (L^2(\Omega))^s, \mathbf{m} \in \mathbf{V}^s} \left\{ \mathcal{E}(\mathbf{u}) + \frac{1}{2\tau} \int_{\Omega} (D_i(x) u_i)^{-1} |\mathbf{m}_i|^2 \, dx \right\} \\
&\quad \text{s.t. } u_i - u_i^k + \nabla \cdot \mathbf{m}_i = 0, \quad i = 1, \dots, s. \\
&\quad -\nabla \cdot (\varepsilon_0 \nabla \varphi) = f(x) + \sum_{i=1}^s z_i u_i,
\end{aligned}$$

where

$$\mathcal{E}(\mathbf{u}) = \int_{\Omega} \sum_{i=1}^s u_i \log u_i + \frac{\varepsilon_0}{2} |\nabla \varphi(x)|^2 \, dx.$$

This optimization problem, with two linear constraints, has been derived in [22] in several steps by approximating a dynamical formulation of the JKO type scheme [17]. Refer to [22] for further details on an alternative derivation, along with other formulations with different boundary conditions for φ .

Example 5: The Maxwell-Stefan problem.

For the Maxwell-Stefan problem, we are led to

$$\begin{aligned}
(\mathbf{u}^{k+1}, \mathbf{m}^{k+1}) &= \operatorname{argmin}_{\mathbf{u} \in (L^2(\Omega))^s, \mathbf{m} \in \mathbf{V}^s} \left\{ \int_{\Omega} \sum_{i=1}^s u_i \log u_i \, dx + \frac{1}{4\tau} \int_{\Omega} \sum_{i,j=1}^s b_{ij} u_i u_j \left| \frac{\mathbf{m}_i}{u_i} - \frac{\mathbf{m}_j}{u_j} \right|^2 \, dx \right\}, \\
&\quad \text{s.t. } u_i - u_i^k + \nabla \cdot \mathbf{m}_i = 0, \quad i = 1, \dots, s; \quad \text{and } \sum_{i=1}^s \nabla \cdot \mathbf{m}_i = 0.
\end{aligned}$$

Such constraint minimization differs yet similar to that discussed in [16], in which the authors formulate an optimization problem for interpreting the implicit-explicit scheme to the Maxwell-Stefan problem.

Again our variational scheme is related to the JKO scheme [17], an analogy due to the connection between frictional dissipation and the Wasserstein distance offered by the Benamou–Brenier interpretation [1] of the Monge–Kantorovich mass transfer problem. There is however one important difference, as the frictional dissipation is more elaborate in the multi-component mixture situation. The minimizers of the above constraint problem can be calculated by considering the min-max augmented Lagrangian, which upon taking $\tau \mathbf{v}_i = \frac{\mathbf{m}_i}{u_i}$ gives

$$\begin{aligned} \min_{\mathbf{u}, \mathbf{v}} \max_{\alpha, \beta} L(\mathbf{u}, \mathbf{v}, \alpha, \beta) &= \int_{\Omega} \sum_{i=1}^s u_i \log u_i + \frac{\tau}{4} \sum_{i,j=1}^s b_{ij} u_i u_j |\mathbf{v}_i - \mathbf{v}_j|^2 \, dx \\ &\quad - \int_{\Omega} \tau \alpha \sum_{i=1}^s \nabla \cdot (\mathbf{v}_i u_i) \, dx - \int_{\Omega} \sum_{i=1}^s (\beta_i (u_i - u_i^k) - \tau \nabla \beta_i \cdot \mathbf{v}_i u_i) \, dx. \end{aligned}$$

Computing the variational derivatives, which vanish at the saddle points, we obtain

$$\begin{aligned} 1 + \log u_i + \frac{\tau}{2} \sum_{j=1}^s b_{ij} u_j |\mathbf{v}_i - \mathbf{v}_j|^2 + \tau \alpha \cdot \mathbf{v}_i - \beta_i + \tau \nabla \beta_i \cdot \mathbf{v}_i &= 0 \\ \sum_{j=1}^s b_{ij} u_j (\mathbf{v}_i - \mathbf{v}_j) + \nabla \beta_i &= -\nabla \alpha. \end{aligned}$$

From the first relation we have

$$\beta_i = 1 + \log u_i + O(\tau),$$

which when substituted into the second relation leads to an implicit time-discretization:

$$\begin{aligned} \frac{u_i - u_i^k}{\tau} + \nabla \cdot (u_i \mathbf{v}_i) &= 0, \quad \text{in } \Omega, \\ \sum_{j=1}^s b_{ij} u_j (\mathbf{v}_i - \mathbf{v}_j) + \nabla \log u_i &= \frac{1}{\sum_{j=1}^s u_j} \sum_{j=1}^s u_j \nabla \log u_j + O(\tau), \quad \text{in } \Omega, \\ \sum_{i=1}^s \nabla \cdot (u_i \mathbf{v}_i) &= 0, \quad \text{in } \Omega. \end{aligned}$$

This is a first order approximation to the explicit-implicit scheme introduced in [16]:

$$\begin{aligned} \frac{u_i - u_i^k}{\tau} + \nabla \cdot (u_i^k \mathbf{v}_i) &= 0, \quad \text{in } \Omega, \\ \sum_{j=1}^s b_{ij} u_j^k (\mathbf{v}_i - \mathbf{v}_j) + \nabla \log u_i &= \frac{1}{\sum_{j=1}^s u_j^k} \sum_{j=1}^s u_j^k \nabla \log u_j, \quad \text{in } \Omega, \\ \sum_{i=1}^s \nabla \cdot (u_i^k \mathbf{v}_i) &= 0, \quad \text{in } \Omega. \end{aligned}$$

Example 6: The incompressible and immiscible multi-phase flow in porous media.

For the multiphase flow in porous media, we can derive a discrete scheme

$$\begin{aligned} (\mathbf{u}^{k+1}, \mathbf{m}^{k+1}) &= \arg \min_{\mathbf{u} \in (L^2(\Omega))^s, \mathbf{m} \in \mathcal{V}^s} \left\{ \int_{\Omega} \phi F(\mathbf{u}) \, dx + \frac{1}{\tau} \int_{\Omega} \sum_{i=1}^s \frac{1}{2} \mathbf{m}_i^\top K_i^{-1} \mathbf{m}_i \, dx \right\} \\ &\quad \text{s.t. } \phi (u_i - u_i^k) + \nabla \cdot \mathbf{m}_i = 0, \quad i = 1, \dots, s, \\ &\quad \sum_{i=1}^s u_i = 1, \end{aligned}$$

where $\mathbf{m} = \tau \mathbf{v}$ and $K_i = K_i(\mathbf{u}^k)$. Here τ is the time step size, with initial data \mathbf{u}^0 satisfying $\sum_{i=1}^s u_i^0 = 1$. When τ is small, the minimizer of the above problem may be unique and satisfies the Euler-Lagrange equation which

is indeed a first order explicit-implicit time discretization of the system (36)-(40) with the explicit value only for $K_i = K_i(\mathbf{u}^k)$. By leveraging the definition of $F(\mathbf{u})$, the constraint $\sum_i^s u_i = 1$, and optimization algorithms applied to the aforementioned problem, we observe that the approximation of u_i inherently preserves bounds. Furthermore, the natural mass conservation for each phase is also ensured.

Example 7: The incompressible and immiscible multi-phase flow in porous media with rock compressibility.

For the multi-phase flow in porous media with rock compressibility, we can derive a discrete scheme as follows:

$$(\phi^{k+1}, \mathbf{u}^{k+1}, \mathbf{m}^{k+1}) = \operatorname{argmin}_{\phi \in L^2(\Omega), \mathbf{u} \in (L^2(\Omega))^s, \mathbf{m} \in \mathbf{V}^s} \left\{ \int_{\Omega} \phi F(\mathbf{u}) \, dx + \int_{\Omega} p_e(\phi - \phi^k) \, dx + \frac{1}{\tau} \int_{\Omega} \sum_{i=1}^s \frac{1}{2} \mathbf{m}_i^{\top} K_i^{-1} \mathbf{m}_i \, dx \right\}$$

$$\text{s.t. } \phi u_i - \phi^k u_i^k + \nabla \cdot \mathbf{m}_i = 0, \quad i = 1, \dots, s,$$

$$\sum_{i=1}^s u_i(\phi - \phi^k) + \sum_{i=1}^s \nabla \cdot \mathbf{m}_i = 0,$$

where $\mathbf{m} = \tau \mathbf{v}$ and $K_i = \lambda_i(\mathbf{u}^k)K(\phi^k)$. The second constraint can also be written as $\sum_{i=1}^s u_i = 1$. The initial data \mathbf{u}^0 satisfying $\sum_{i=1}^s u_i^0 = 1$. We apply $\phi = \phi_r e^{\gamma(p_e - p_r)}$ and $K = K_0 \frac{\phi^3(1-\phi_r)^2}{\phi_r^3(1-\phi)^2}$ in the above optimization problem. Thus when τ is small, the minimizer of the above problem may be unique and satisfies the Euler-Lagrange equation which is a first order explicit-implicit time discretization of the nonlinear system (44)-(50) with the explicit value only for $K_i = \lambda_i(\mathbf{u}^k)K(\phi^k)$. The preservation of bounds for u_i and mass conservation for each phase are also maintained through the approximation of the aforementioned minimization problem.

4 Numerical solutions

The core idea of our numerical schemes is to discretize each semi-discrete variational formulation in space, and then apply an efficient algorithm to optimize the problem. It suffices to describe the discretization of the first step, from the datum \mathbf{u}^0 to the minimizer \mathbf{u}^1 .

4.1 The discretized conserved problem

We consider only the general problem with mass conservation,

$$(\mathbf{u}^1, \mathbf{m}^1) = \operatorname{argmin}_{\mathbf{u} \in (L^2(\Omega))^s, \mathbf{m} \in \mathbf{V}^s} \left\{ \frac{1}{\tau} \Phi_{\tau}^0(\mathbf{u}, \mathbf{m}) + \mathcal{E}(\mathbf{u}) \right\}, \quad (58)$$

$$\text{s.t. } u_i - u_i^0 - \nabla \cdot \mathbf{m}_i = 0. \quad (59)$$

We shall use either finite difference or finite element for spatial discretization depending on the domain setup.

Finite difference:

Let the domain be a box $\Omega = [0, 1]^d$, functions on Ω extend periodically. For simplicity, we explain the discretization in $d = 1$ space dimensions, the translation to $d > 1$ is straightforward but notationally cumbersome. We use a cartesian grid with N cells $I_j = [x_{j-1/2}, x_{j+1/2}]$, with uniform grid step $h = 1/N$ and cell center $x_j = x_{j-1/2} + 0.5h$, for $j = 1, \dots, N$. Functions w are discretized by finite sequences $(w_j)_{j=1, \dots, N}$ with $w_j \sim w(x_j)$. We define the difference operator by

$$(D_h w)_{j+1/2} = \frac{w_{j+1} - w_j}{h}, \quad (d_h w)_j = \frac{w_{j+1/2} - w_{j-1/2}}{h}$$

and average by

$$\hat{w}_j = \frac{w_{j+1/2} + w_{j-1/2}}{2}.$$

With these notations, the variational scheme for FPE is now discretized as follows:

$$\min_{u,m} L_h(u, m) := \left\{ \frac{h}{2\tau} \sum_{j=1}^N \frac{|\hat{m}_j|^2}{u_j} + h \sum_{j=1}^N \beta^{-1} u_j \log u_j + u_j U(x_j) \right\},$$

$$s.t. \quad u_j - u_j^0 + (d_h m)_j = 0.$$

For other application examples, the discrete objective function can be similarly obtained.

Finite element:

We can also employ the finite element method for spatial discretization. Let \mathcal{T}_h represent a regular triangulation of Ω with mesh size h . Let U_h and V_h are proper finite element spaces for $u_{h,i}$ and \mathbf{m}_i , respectively. Notice that V_h is a finite element space for vector-valued functions. Then the fully discrete problem is defined as follows,

$$(\mathbf{u}_h^1, \mathbf{m}_h^1) = \operatorname{argmin}_{\mathbf{u}_h \in (U_h)^s, \mathbf{m}_h \in (V_h)^s} \left\{ \frac{1}{\tau} \Phi_\tau^0(\mathbf{u}_h, \mathbf{m}_h) + \mathcal{E}(\mathbf{u}_h) \right\}, \quad (60)$$

$$s.t. \quad \int_{\Omega} (u_{h,i} - u_{h,i}^0 - \nabla \cdot \mathbf{m}_{h,i}) v_h dx = 0, \quad \forall v_h \in U_h.$$

In applications, we can choose the finite element spaces so that the fully discrete system is well-posed.

4.2 Solution by optimization algorithms

In this section, we delve into numerical techniques for solving the constraint optimization problem denoted by (57). Let $\theta = (u, m)$, then the problem takes the form

$$\min_{\theta} L_h(\theta), \quad \text{subject to } B\theta = b, \quad (61)$$

where $L_h \in C^1(\mathbb{R}^n)$ is bounded below, the constraint set is the linear system corresponding to the discretized PDE constraints. $B \in M^{l \times n}$ is a matrix with $l \leq n$ and $b \in \mathbb{R}^l$ is a vector. A straightforward method to tackle this constraint optimization is through the following update:

$$\theta_{k+1} = \theta_k - \eta G \nabla L_h(\theta_k), \quad (62)$$

where the projection matrix G is defined by

$$G = I - B^\top (BB^\top)^{-1} B,$$

ensuring $B\theta_{k+1} = b$ if $B\theta_k = b$. Here, η is a step size (or learning rate), crucial for the algorithm's convergence due to the gap between the continuous gradient flow equation and the discrete iteration. Typical choices for η are either empirical schedules or damping techniques.

For enhanced efficiency, we also employ the AEPG algorithm (adaptive energy-based preconditioned gradient descent) introduced in [23], which reads:

$$v_k = G \nabla l(\theta_k), \quad (63a)$$

$$r_{k+1} = \frac{r_k}{1 + 2\eta \|v_k\|^2}, \quad (63b)$$

$$\theta_{k+1} = \theta_k - 2\eta r_{k+1} v_k, \quad (63c)$$

where $l(\theta) = \sqrt{L_h(\theta) + c}$, $c \in \mathbb{R}$ such that $\inf_{\theta \in \Theta} (L(\theta) + c) > 0$, and $\eta > 0$ is the base step size. One striking feature of this algorithm is its unconditional energy stability, i.e., r_k as an approximation of $\sqrt{L_h + c}$ is decreasing in k for any $\eta > 0$. Consult [23] for further details of this algorithm.

In certain model scenarios where computational complexity is not prohibitive, its feasible to directly tackle the corresponding Euler-Lagrange equation using iterative methods. In such cases, the problem (61) transforms into a nonlinear equation with a Lagrange multiplier λ :

$$\begin{aligned}\nabla L_h(\theta) + B^\top \lambda &= 0, \\ B\theta &= b.\end{aligned}$$

We assume that B satisfies the inf-sup condition, ensuring the well-posedness of the above problem. A standard Newton scheme for solving the nonlinear equation can be expressed as:

$$\begin{pmatrix} \theta^{k+1} \\ \lambda^{k+1} \end{pmatrix} = \begin{pmatrix} \theta^k \\ \lambda^k \end{pmatrix} - \begin{pmatrix} \nabla^2 L_h(\theta^k) & B^\top \\ B & 0 \end{pmatrix}^{-1} \begin{pmatrix} \nabla L_h(\theta^k) + B^\top \lambda^k \\ B\theta^k - b \end{pmatrix}. \quad (64)$$

Remark 2 *The optimization algorithms described above offer flexibility in space discretizations. For instance, when employing the mixed finite element method to solve two-phase flow in porous media, as demonstrated in Example 6 and Example 7, conventional approaches require the use of upwind schemes in space discretization for mass conservation equations via semi-implicit schemes [20, 19]. However, with the optimization algorithms outlined, we find that the imposition of upwind schemes in the space discretization of mass conservation equations is unnecessary. Its worth noting a recent advancement in [25], presenting a novel approach for numerically solving time-dependent conservation laws using implicit schemes via primal-dual hybrid gradient methods. In our research, we focus on using the Onsager variational principle as an approximation tool, wherein the minimization of the discrete Rayleighian functional is achieved through optimization algorithms.*

4.3 Simulations

The numerical experiments for single equations can be found in literature. We present only some examples for PNP and the two-phase porous media equations. They include more than one component.

In the following numerical experiments, we choose the finite element method and implement the schemes in Netgen/NGSolve([34, 35]). We choose to use the method (64) to solve the optimization problem (61) in the numerical experiments below.

Example 1. In the first example, we consider the PNP equation in a square region $(0, 1) \times (0, 1)$. The periodic boundary conditions are proposed for the system. Assume there exist two components in the system and one has positive charges and the other has negative charges. The initial distributions are given respectively by $u_1 = 1.02 + \sin(2\pi x) * \cos(2\pi x)$ and $u_2 = 1.02 + \sin(2\pi y) * \cos(2\pi y)$. We would like to compute the evolution of the two components.

We partition the domain uniformly with mesh size $h = 0.05$. We use P_2 finite elements to discretize u_i and λ_i , and use P_3 finite elements for \mathbf{m}_i and ϕ_i . We set $\tau = 0.0001$. We use the scheme in the previous section. To solve the problem. In each time step, we use a Newton method to solve the nonlinear algebraic equation. It turns out the Newton method converges fast and only two or three iterations are needed in each time step. The discrete solution is shown in Figure 1. We could see that the distributions of the two ions become more and more homogeneous due to the diffusion. In Figure 2, we show the change of the total energy with respect to time. We could see that the energy always decays. This verifies the theoretical analysis in Proposition 2 in Section 3. In Figure 3, we show the change of the total mass of the two components with respect to time. We could see that the total mass for each component keeps constant.

Example 2. In this example, we consider two-phase flow in porous media within a closed system in a square region $[0, 100 \text{ m}]^2$ with constant porosity. We utilize the data as in [20]. The initial distribution of wetting-phase saturation and permeability are illustrated in Figure 4. In a porous medium, the porosity in the high-permeability

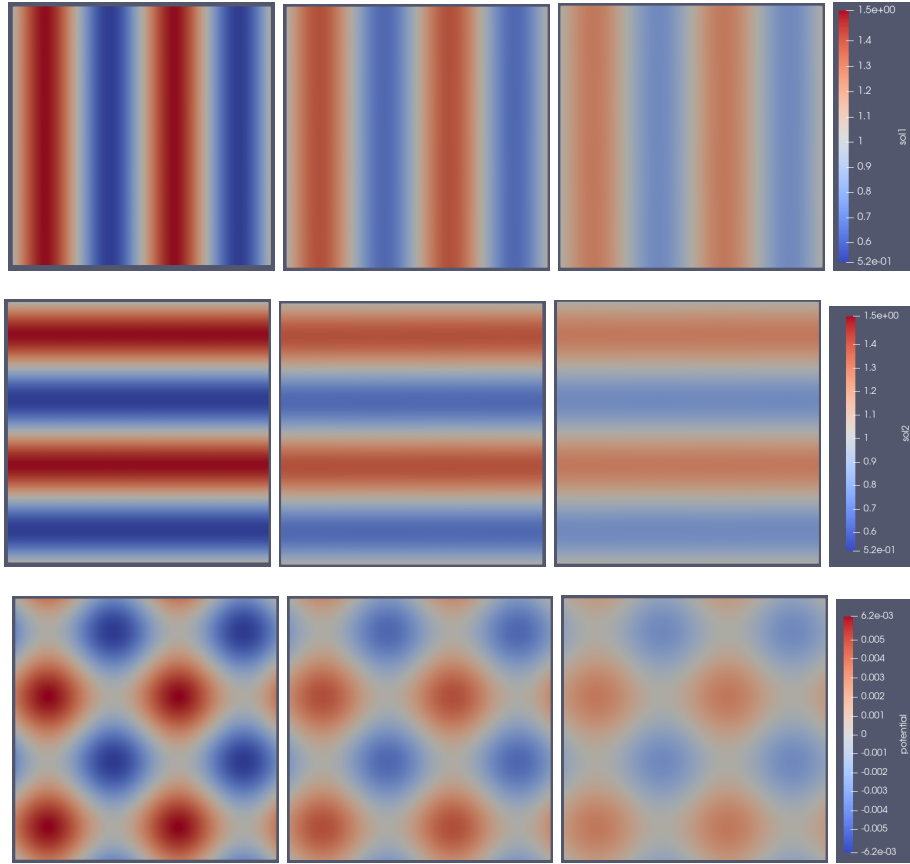


Figure 1: The solutions of the PNP equation. First Row: the distribution of u_1 at various time $t = 0.0005, 0.0025, 0.005$; Second Row: the distribution of u_2 at various time $t = 0.0005, 0.0025, 0.005$; Last Row: the potential ψ at various time $t = 0.0005, 0.0025, 0.005$.

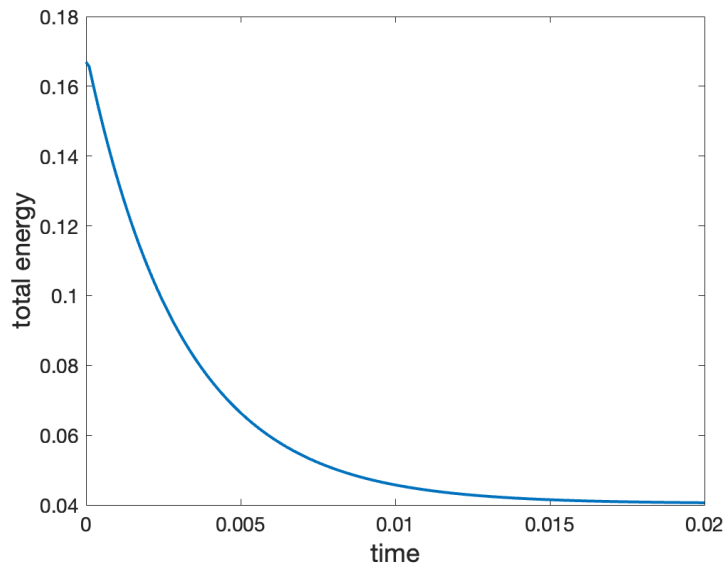


Figure 2: The change of the total energy with respect to time

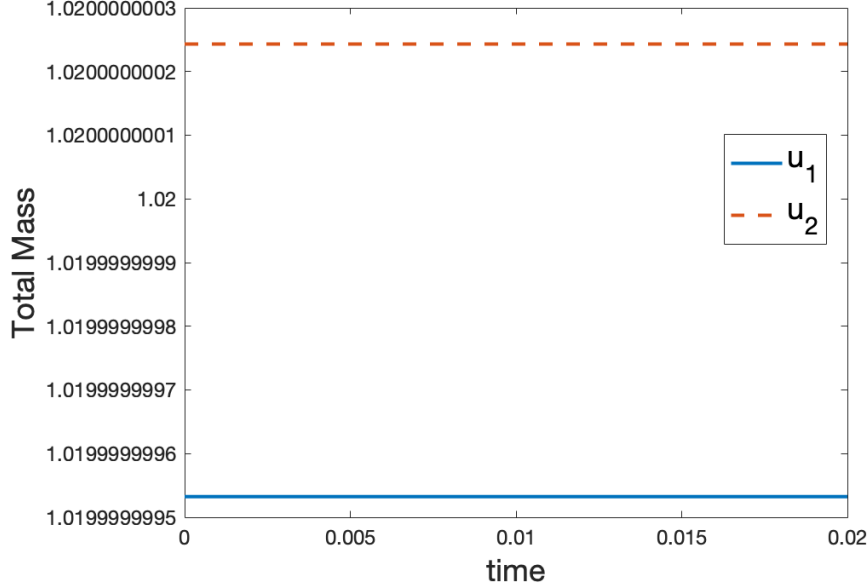


Figure 3: The change of the total mass of the two components with respect to time

region is 0.3, while the porosity in the rest region is 0.15. The energy parameter in the high-permeability region are given as $\gamma_w = 11.655$ bar, $\gamma_n = 1.0796$ bar, $\gamma_{wn} = 7.424$ bar, while the energy parameter in the low-permeability region are $\gamma_w = 5.8275$ bar, $\gamma_n = 0.5398$ bar, $\gamma_{wn} = 3.721$ bar. The viscosities are taken as $\eta_w = 0.9$ cP and $\eta_n = 0.1$ cP, respectively.

The relative permeability is obtained from the following equation:

$$k_{rw}(S_w) = S_w^3, \quad k_{rn} = (1 - S_w)^3.$$

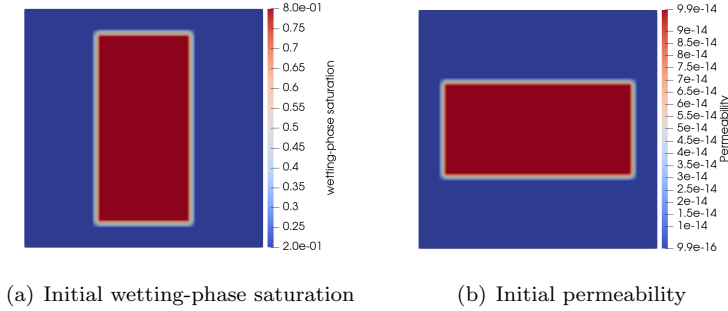


Figure 4: Initial distributions of wetting-phase saturation and permeability in Example 2.

We use the uniform mesh with 60×60 grid cells, the time step size is taken as $\tau = 0.01$ day. Figure 5 shows that the total free energy is monotonously decreasing with time. The saturation distribution at different times is shown in Figure 6. In this closed system, the chemical potential gradient becomes a dominant driving force. The pressure and chemical potential contours are illustrated in Figure 7 and 8. The numerical results coincide with the results in [20].

Example 3. In this example, we simulate a two-phase flow in porous media with rock compressibility. The problem is considered in a closed system within the square region $[0, 10 \text{ m}]^2$. We utilize the data as in [19]. The initial distributions of porosity and permeability are illustrated in Figure 9. We take the reference porosity $\phi_r = 0.175$.

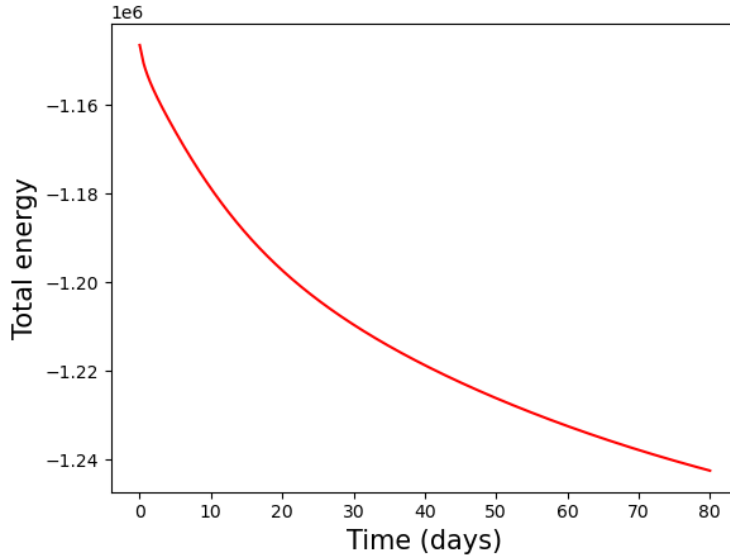


Figure 5: Energy dissipation with time in Example 2.

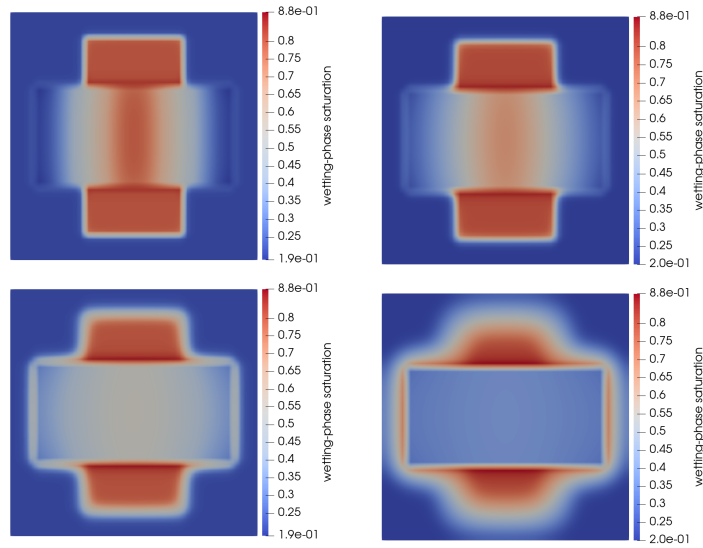


Figure 6: Distributions of wetting-phase saturation at different times in Example 2. Top-left: $t = 5$ days. Top-right: $t = 10$ days. Bottom-left: $t = 20$ days. Bottom-right: $t = 80$ days.

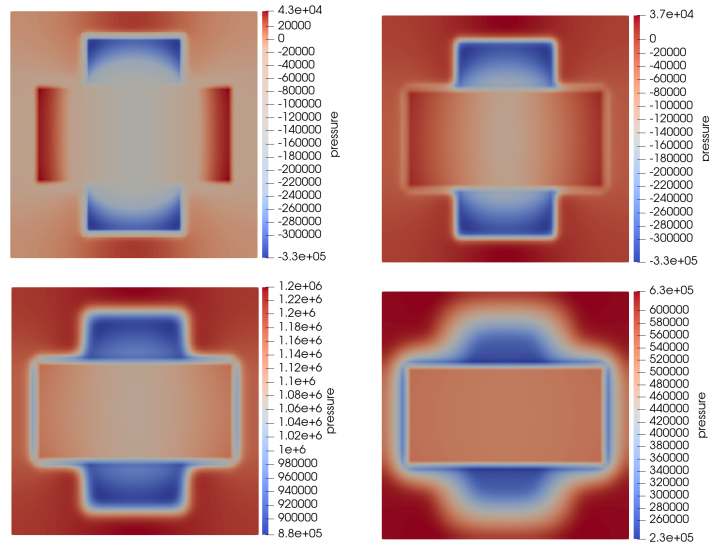


Figure 7: Distributions of pressure at different times in Example 2. Top-left: $t = 5$ days. Top-right: $t = 10$ days. Bottom-left: $t = 20$ days. Bottom-right: $t = 80$ days.

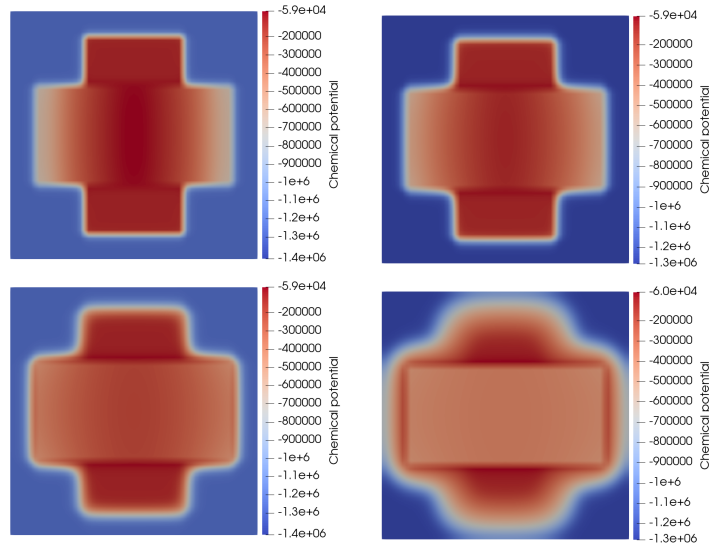


Figure 8: Distributions of chemical potential of wetting-phase at different times in Example 2. Top-left: $t = 5$ days. Top-right: $t = 10$ days. Bottom-left: $t = 20$ days. Bottom-right: $t = 80$ days.

The viscosities are taken as $\eta_w = 1$ cP and $\eta_n = 0.5$ cP, respectively. For the energy parameters, we take

$$\sigma_w = \frac{\bar{\sigma}_w}{\sqrt{K_0}}, \quad \sigma_n = \frac{\bar{\sigma}_n}{\sqrt{K_0}}, \quad \sigma_{wn} = \frac{\bar{\sigma}_{wn}}{\sqrt{K_0}}, \quad \sigma_{ws} = \sigma_{ns} = 0.$$

In this example, we take $\bar{\sigma}_w = 0.58$ Pa, $\bar{\sigma}_n = 0.05$ Pa, $\bar{\sigma}_{wn} = 0.36$ Pa, and the relative permeability is given as that in Example 2. We initialize the wetting-phase and non-wetting-phase saturation with a uniform distribution, setting $S_w^0 = 0.3, S_n^0 = 0.7$. In this example, we simulate the problem in a uniform mesh with 70×70 grid cells and the time step size is taken as $\tau = 0.001$ day.

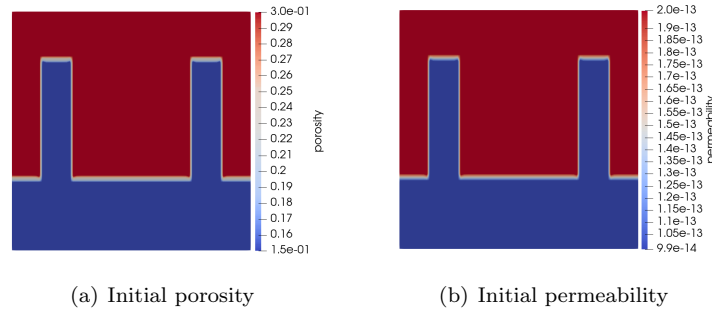


Figure 9: Initial distributions of porosity and permeability in Example 3.

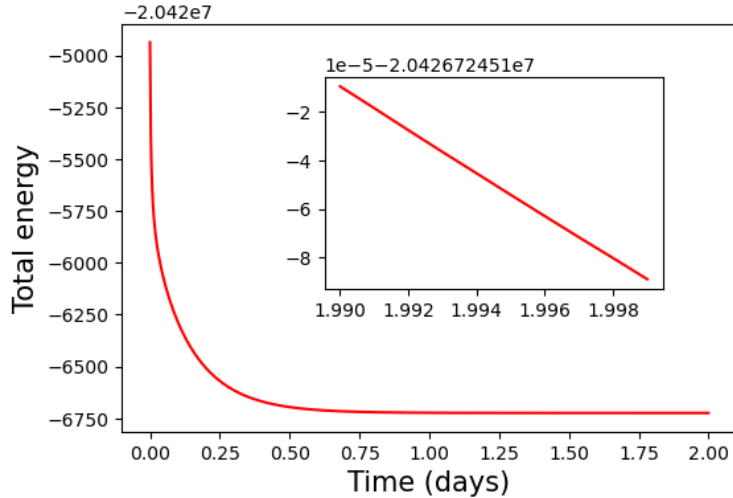


Figure 10: Energy dissipation with time in Example 3.

Figure 10 depicts the total free energy decreases monotonically with time until a steady state is reached. In Figure 11, we illustrate the wetting-phase saturation fluid flows from high-permeability regions to low-permeability regions until an equilibrium state is reached. As shown in Figure 12 and Figure 13, the effective pore pressure significantly increases in the low-permeability region, leading to an increase in the porosity of the original low-permeability region and a decrease in the porosity of the remaining regions. The numerical results also coincide with the results in [19].

5 Conclusion

In conclusion, we introduce a novel framework for designing physics-preserving numerical schemes applicable to a wide range of dissipative systems. Our approach centres on leveraging the Onsager variational principle as an

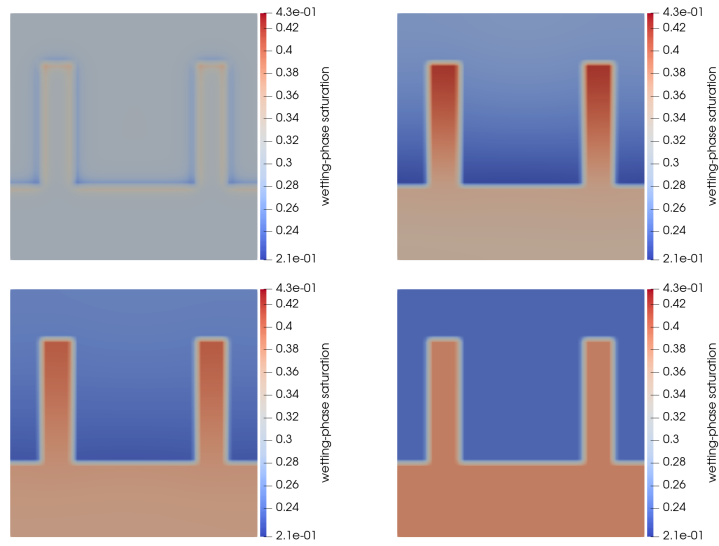


Figure 11: Distributions of wetting-phase saturation at different times in Example 3. Top-left: $t = 0.1$ day. Top-right: $t = 0.2$ day. Bottom-left: $t = 0.5$ day. Bottom-right: $t = 2$ days.

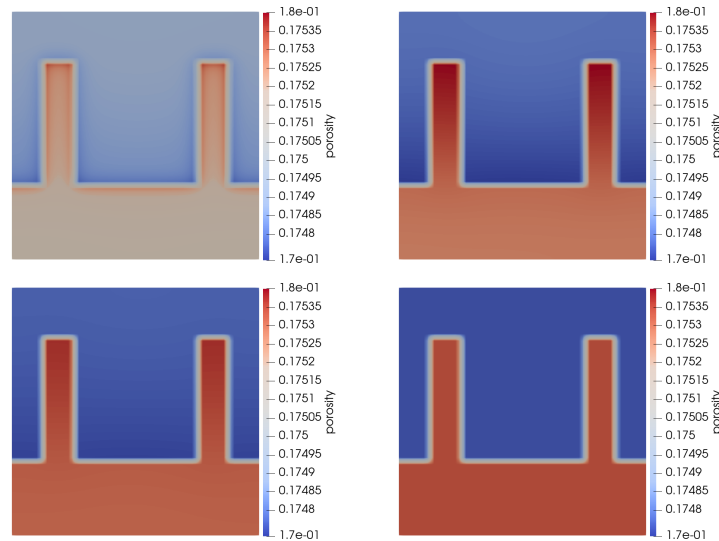


Figure 12: Distributions of porosity at different times in Example 3. Top-left: $t = 0.1$ day. Top-right: $t = 0.2$ day. Bottom-left: $t = 0.5$ day. Bottom-right: $t = 2$ days.

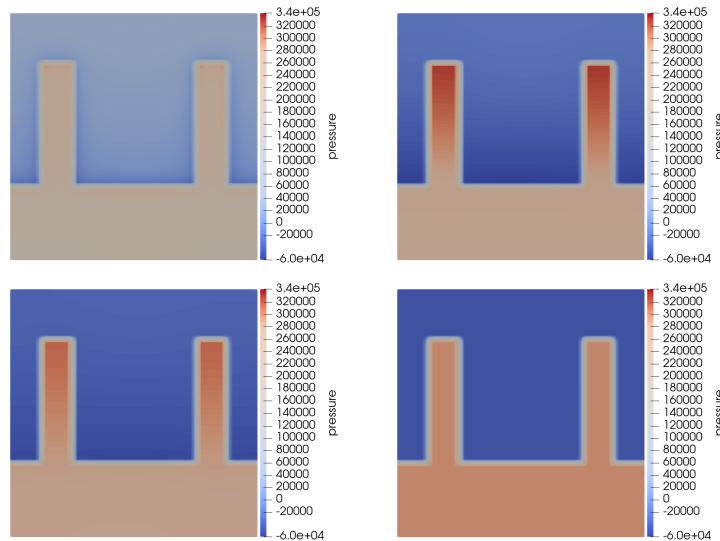


Figure 13: Distributions of effective pressure at different times in Example 3. Top-left: $t = 0.1$ day. Top-right: $t = 0.2$ day. Bottom-left: $t = 0.5$ day. Bottom-right: $t = 2$ days.

approximation tool. Initially, we show that the Onsager principle yields essential dynamic equations for both conservative and non-conservative quantities, including notable examples such as phase field equations (e.g., the Allen-Chan or Cahn-Hilliard equations), the Fokker-Planck equation, the PNP equation, and equations governing porous media flows, etc. Subsequently, we illustrate how this variational principle offers a natural and unified methodology for deriving discrete-time schemes tailored to these equations. These schemes are founded upon the minimization of the discrete Rayleighian functional. While some schemes align with some existing methods like the JKO scheme in specific scenarios. However, direct application of the JKO scheme is uncommon due to the computational challenges associated with computing Wasserstein distances. Our analysis demonstrates that our schemes uphold crucial system properties such as mass conservation and energy dissipation structures. Moreover, our approach allows for flexible spatial discretization choices. We provide numerical experiments to validate the effectiveness of our method.

References

- [1] J.-D. Benamou and Y. Brenier. A computational fluid mechanics solution to the Monge-Kantorovich mass transfer problem. *Numer. Math.*, 84(3):375–393, 2000.
- [2] G. Beylkin, J. M. Keiser, and L. Vozovoi. A new class of time discretization schemes for the solution of nonlinear pdes. *J. Comput. Phys.*, 147:362–387, 1998.
- [3] X. Chen, X.-P. Wang, and X. Xu. Analysis of the Cahn–Hilliard equation with a relaxation boundary condition modeling the contact angle dynamics. *Archive for Rational Mechanics and Analysis*, 213(1):1–24, 2014.
- [4] S. M. Cox and P. C. Matthews. Exponential time differencing for stiff systems. *J. Comput. Phys.*, 176:430–455, 2002.
- [5] Ennio De Giorgi. Movimenti minimizzanti. In *Aspetti e problemi della Matematica oggi, Proc. of Conference held in Lecce*, 1992.
- [6] M. Doi. *Soft Matter Physics*. Oxford University Press, Oxford, 2013.
- [7] M. Doi. Onsager principle as a tool for approximation. *Chin. Phys. B*, 24:020505, 2015.

- [8] Q. Du, L. Ju, X. Li, and Z. Qiao. Maximum bound principles for a class of semilinear parabolic equations and exponential time-differencing schemes. *SIAM Review*, 63:317–359, 2021.
- [9] C. Duan, W. Chen, C. Liu, X. Yue, and S. Zhou. Structure-preserving numerical methods for nonlinear Fokker-Planck equations with nonlocal interactions by an energetic variational approach. *SIAM J. Sci. Comput.*, 43:B82–B107, 2021.
- [10] B. Eisenberg, Y. Hyon, and C. Liu. Energy variational analysis of ions in water and channels: field theory for primitive models of complex ionic fluids. *J. Chem. Phys.*, 133:104104, 2010.
- [11] D. J. Eyre. Unconditionally gradient stable time marching the Cahn-Hilliard equation. *Mater. Res. Soc. Sympos. Proc.*, pages 39–46, 1998.
- [12] H. Gao, J. Kou, S. Sun, and X. Wang. Thermodynamically consistent modeling of two-phase incompressible flows in heterogeneous and fractured media. *Oil Gas Sci. Technol., Rev. IFP Énerg. Renov.*, 75:32, 2020.
- [13] M. Hochbruck and A. Ostermann. Explicit exponential Runge-Kutta methods for semilinear parabolic problems. *SIAM J. Numer. Anal.*, 43:1069–1090, 2005.
- [14] J. Hu and X. Huang. A fully discrete positivity-preserving and energy-dissipative finite difference scheme for Poisson-Nernst-Planck equations. *Numer. Math.*, 145:77–115, 2020.
- [15] F. Huang and J. Shen. Bound/positivity preserving and energy stable scalar auxiliary variable schemes for dissipative systems: Applications to Keller-Segel and Poisson-Nernst-Planck equations. *SIAM J. Sci. Comput.*, 43:A1832–A1857, 2021.
- [16] X. Huo, H. Liu, A. E. Tzavaras, and S. Wang. An energy stable and positivity-preserving scheme for the Maxwell–Stefan diffusion system. *SIAM J. Numer. Anal.*, 59(5):2321–2345, 2021.
- [17] R. Jordan, D. Kinderlehrer, and F. Otto. The variational formulation of the Fokker-Planck equation. *SIAM Journal on Mathematical Analysis*, 29(1):1–17, 1998.
- [18] L. P. Kadanoff. *Statistical Physics: Statics, Dynamics and Renormalization*. World Scientific, 2000.
- [19] J. Kou, X. Wang, H. Chen, and S. Sun. An energy stable, conservative and bounds-preserving numerical method for thermodynamically consistent modeling of incompressible two-phase flow in porous media with rock compressibility. *Int. J. Numer. Methods Eng.*, 124:2589–2617, 2023.
- [20] J. Kou, X. Wang, S. Du, and S. Sun. An energy stable linear numerical method for thermodynamically consistent modeling of two-phase incompressible flow in porous media. *J. Comp. Phys.*, 451:110854, 2022.
- [21] C. Liu, C. Wang, S. Wise, X. Yue, and S. Zhou. A positivity-preserving, energy stable and convergent numerical scheme for the Poisson-Nernst-Planck system. *Math. Comp.*, 90:2071–2106, 2021.
- [22] H. Liu and W. Maimaitiyiming. A dynamic mass transport method for Poisson-Nernst-Planck equations. *Journal of Computational Physics*, 473:111699, 2023.
- [23] H. Liu, L. Nurbekyan, X. Tian, and Y. Yang. Adaptive preconditioned gradient descent with energy. *arXiv preprint, arXiv:2310.06733*, 2023.
- [24] H. Liu and Z. Wang. A free energy satisfying discontinuous Galerkin method for one-dimensional poisson-nernst-planck systems. *J. Comput. Phys.*, 328:413–437, 2017.
- [25] S. Liu, S. Osher, W. Li, and C.-W. Shu. A primal-dual approach for solving conservation laws with implicit in time approximations. *J. Comp. Phys.*, 472:111654, 2023.
- [26] Y. Liu and X. Xu. A variational discretization method for mean curvature flows by the Onsager principle. *arXiv preprint, arXiv:2404.11935*, 2024.

- [27] S. Lu and X. Xu. An efficient diffusion generated motion method for wetting dynamics. *J. Comput. Phys.*, 441:110476, 2021.
- [28] X. Man and M. Doi. Ring to mountain transition in deposition pattern of drying droplets. *Phys. Rev. Lett.*, 116:066101, 2016.
- [29] L. Onsager. Reciprocal relations in irreversible processes. I. *Phys. Rev.*, 37(4):405–426, 1931.
- [30] L. Onsager. Reciprocal relations in irreversible processes. II. *Phys. Rev.*, 38(12):2265–2279, 1931.
- [31] A. Prohl and M. Schmuck. Convergent discretizations for the Nernst–Planck–Poisson system. *Numer. Math.*, 111:591–630, 2009.
- [32] Y. Qian, C. Wang, and S. Zhou. A positive and energy stable numerical scheme for the Poisson-Nernst-Planck-Cahn-Hilliard equations with steric interactions. *J. Comput. Phys.*, 426:109908, 2021.
- [33] H. Risken and H. Risken. *Fokker-Planck Equation*. Springer, 1996.
- [34] J. Schöberl. Netgen an advancing front 2D/3D-mesh generator based on abstract rules. *Computing and visualization in science*, 1(1):41–52, 1997.
- [35] J. Schöberl. C++ 11 implementation of finite elements in NGSolve. *Institute for analysis and scientific computing, Vienna University of Technology*, 30, 2014.
- [36] J. Shen, C. Wang, X. Wang, and S. M. Wise. Second-order convex splitting schemes for gradient flows with Ehrlich-Schwoebel type energy: application to thin film epitaxy. *SIAM J. Numer. Anal.*, 50:105–125, 2012.
- [37] J. Shen, J. Xu, and J. Yang. The scalar auxiliary variable (SAV) approach for gradient flows. *J. Comput. Phys.*, 353:407–416, 2018.
- [38] J. Shen, J. Xu, and J. Yang. A new class of efficient and robust energy stable schemes for gradient flows. *SIAM Review*, 61:474–506, 2019.
- [39] J. Shen, X. Yang, and H. Yu. Efficient energy stable numerical schemes for a phase field moving contact line model. *J. Comput. Phys.*, 284:617–630, 2015.
- [40] S. Xiao and X. Xu. A moving mesh method for porous medium equation by the Onsager variational principle. *arXiv preprint, arXiv:2403.20030*, 2024.
- [41] C. Xu and T. Tanng. Stability analysis of large time-stepping methods for epitaxial growth models. *SIAM J. Numer. Anal.*, 44:1759–1779, 2006.
- [42] X. Xu. A variational analysis for the moving finite element method for gradient flows. *J. Comput. Math.*, 41(2):191–210, 2023.
- [43] X. Xu, Y. Di, and M. Doi. Variational method for contact line problems in sliding liquids. *Phys. Fluids*, 28:087101, 2016.
- [44] X. Yang and L. Ju. Efficient linear schemes with unconditional energy stability for the phase field elastic bending energy model. *Comput. Methods Appl. Mech. Engrg.*, 315:691–712, 2017.
- [45] J. Zhao, X. Yang, Y. Gong, and Q. Wang. A novel linear second order unconditionally energy stable scheme for a hydrodynamic Q-tensor model of liquid crystals. *Comput. Methods Appl. Mech. Engrg.*, 318:803–825, 2017.